# ARTICLE

# DETECTION AND RECONSTRUCTION OF RADAR FOOT PRINTS FOR MAP UPDATING

G.Vijayalakshmi[1], B. Sathyasri [2], V.Mahalakshmi[3] M. Anto Bennet[4*]

*Electronics and Communication Engineering, VEL TECH ,Avadi,Chennai 600 062, Tamil Nadu, INDIA*

## ABSTRACT

*The space borne synthetic aperture radar systems acquires imagery with very high spatial resolution, supporting various important application scenarios, such as damage assessment in urban areas after natural disasters. To ensure a reliable, consistent, and fast extraction of the image from the complex synthetic aperture radar scenes. Focusing on the analysis of urban areas, which is of the prime interest of VHR SAR. In this work we proposed a normal method for the automatic detection and 2-D reconstruction of radar foot prints. The method is based on the extraction of a set of low-level features from the images and on their composition to more structured primitives using a production system. The semantic meaning represents the probability that a primitive belongs to a certain scattering class and has been defined in order to compensate for the lack of detectable features in images. The efficiency of the proposed method is demonstrated by processing a 1-m resolution TerraSAR-X spot beam scene containing flat and gable-roof buildings at various settings. The results show that the method has a high overall detection rate and that radar foot prints are well reconstructed, in particular for medium and large buildings.*

## INTRODUCTION

In the last decade, very high spatial resolution (VHR) space borne remote sensing sensors acquiring data with meter or sub-meter resolutions became widely available. These data have the potential to be employed for various important application scenarios, such as the monitoring of changes in urban areas, the characterization of urban areas, the surveillance of the effects of violent conflicts, and the crisis management after natural disasters. For the latter application scenario, space borne VHR synthetic aperture radar (SAR) sensors, such as Cosmo-SkyMed and TerraSAR-X, are of particular interest, due to their independence on the solar illumination and the relative insensitivity to the weather conditions. One of the main drawbacks of VHR SAR is the complexity of the images, mainly owing to the speckle effect and the side looking geometry of the SAR sensor, hampering the interpretation of the data by non-SAR experts. This is particularly true for urban areas, where the data are mainly characterized by layover, multi bounce, and shadowing effects of the buildings.

Therefore, to support the widespread usage of VHR SAR, robust automatic information extraction methods are essential. Different techniques for building detection and reconstruction from VHR SAR images have been presented in literature. The developed method uses a tree of hypotheses, which is simplified according to a set of semantic rules. The approach is based on the detection of edges and their combination to building footprints. A method for the extraction of buildings and the estimation of their height from stereoscopic airborne radar images while a building extraction method using dual aspect SAR data was presented. An algorithm for building reconstruction from multi-aspect polarimetric SAR (PolSAR) images. The polarimetric information is exploited by employing an edge detector effective on polarimetric images. The retrieved edges are then parameterized by means of the Hough transform to generate the building footprint hypotheses. Another method based on shadow analysis which exploits InSAR data and is suitable for high or isolated buildings. A building detection method using an orthophoto and an InSAR image based on conditional random Techniques for the 3-D reconstruction of buildings using VHR optical data for the 2-D building footprint reconstruction and a single VHR SAR scene for the building height extraction. All the aforementioned works addressed the problem of building detection and reconstruction in VHR SAR images by relying on the availability of ancillary or multi-sensor data, PolSAR, InSAR, or multidimensional airborne data which implies that the area under investigation is imaged more than once with different viewing configurations. This represents a limitation for application scenarios with stringent timing restrictions that do not allow the acquisition of multidimensional SAR data. For these reasons, research on the detection and extraction of buildings from single VHR SAR data is important. This method fails in the detection of buildings if they do not show L-shaped returns. Moreover, it considers only bright lines and discards other relevant features, such as bright areas and shadows. We propose a novel method for the detection and reconstruction of building radar footprints from detected VHR SAR images. Unlike most of the literature methods, it can be applied to single images. Moreover, it is suitable to be used with data acquired by currently operational space borne SAR sensors. In this context, radar footprint refers to the characteristic scattering signature of buildings in SAR. The method integrates the concepts of basic feature extraction and their composition to more structured primitives using a production system. In order to compensate for the lack of detectable features in single images, the concept of semantic meaning of the primitives is introduced and used to generate building candidates and reconstruct radar footprints. The semantic meaning represents the probability that a primitive belongs to a certain scattering class and allows the selection of the most reliable primitives and footprint hypothesis on the basis of fuzzy

**\*Corresponding Author**
Email:
bennetmab@gmail.com

111

membership grades. In addition, as shown later in the project, the method is suited to the implementation on computer clusters, thereby making it possible almost-real-time applications. Since their approach relies on sub meter-resolution InSAR data, the hypotheses are based on different information compared to ours. Moreover, we introduce a way to quantitatively evaluate the hypotheses to automatically select the best one, however, this method is based on a global MAP estimation using Monte Carlo methods, while the approach proposed in this project exploits also the shadow information and introduces the concept of semantic meaning and membership grade for each primitive and footprint hypothesis. Moreover, such a work was intended as a tool for the investigation of the limits and merits of information extraction from single images, and was not optimized for building reconstruction purposes. The radar footprint map extracted with the proposed method can be used to derive different information, such as the buildup presence index.

## LITERATURE SURVEY

This paper proposes a novel method for the detection and reconstruction of building radar footprints from detected VHR SAR images. Unlike most of the literature methods, it can be applied to single images. Moreover, it is suitable to be used with data acquired by currently operational space borne SAR sensors. In this context, radar footprint refers to the characteristic scattering signature of buildings in SAR. The method integrates the concepts of basic feature extraction and their composition to more structured primitives using a production system. In order to compensate for the lack of detectable features in single images, the concept of semantic meaning of the primitives is introduced and used to generate building candidates and reconstruct radar footprints.The efficiency of the proposed method is demonstrated by processing a 1-m resolution TerraSAR-X spotbeam scene containing flatand gable-roof buildings at various settings.The results show that the method has a high overall detection rate and that radar footprints are well reconstructed, in particular for medium and large buildings[1,5].

Imaging radar has recently become available at geometric resolutions high enough to begin thinking about mapping of individual buildings with their 3-dimensional shapes. This is based on interferometric elevation data as well as magnitude images with their shadows and layover representations from vertical objects. We discuss how an automated procedure can build models of buildings at an accuracy of 1 meter, given radar images with pixel diameters of 30 cms [2,6].

2.5D building modelling is of great interest for visualization, simulation and monitoring purposes in different cases like city and military mission planning or rapid disaster assessment. Manual and automatic extraction of building information from SAR interferometry is complicated by layover, foreshortening, shadowing and multi-bounce scattering, especially in dense urban areas with tall buildings. This can be overcome by using optical imagery to provide the shapes of the building footprints whereas SAR data is used for the refinement of the detected footprints and for providing building height information. In conclusion, building height from SAR interferometry can improve building footprint extraction from optical images and can be combined with the extracted footprints to generate a 2.5D building model [3,7].

 In this project we present a novel method for automatic building detection, which also reconstructs the 2D radar footprint of the detected buildings. The method is based on the extraction of a set of low-level features from the images and on their combination in more structured primitives. Then the semantic meaning of primitives is used for the definition of building candidates and for the radar footprint reconstruction. In order to process large VHR SAR images, the method has been implemented on a computer cluster. We demonstrate the effectiveness of the method using a large TerraSAR-X spotlight scene [4, 8].

### Proposed method

The proposed technique for the automatic detection and reconstruction of building radar footprints from single VHR SAR images is suited for meter-resolution data.The radar footprints corresponding to very tall buildings have a high probability to be detected.The algorithm does not require the buildings to be isolated, such buildings usually show a clear shadow feature, which is exploited by the algorithm to improve the detection performance.

### Modeling of building footprints

The key characteristics of buildings in SAR are the layover, double-bounce, and shadowing effects which are caused by the side-looking and ranging properties of SAR sensors. To illustrate this schematic view of the scattering profile of a simplified flat-roof building model shown in [Fig. 1].
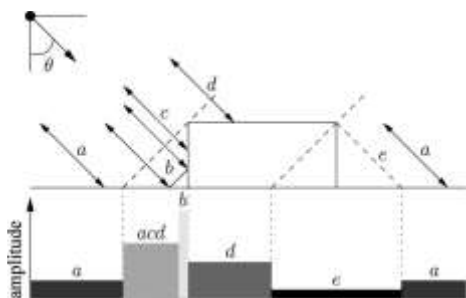
**Fig. 1:** Scattering model for a flat-roof building with viewing directionfrom left.

………………………………………………………………………………………

The building in the middle, which is modeled as a rectangular box, is imaged by a sensor with incidence angle θ. The annotations a refer to backscattering from the ground surface surrounding the building. acd denotes the layover area where scattering from the ground, from the vertical building front wall and from parts of the flat roof are superimposed since these parts have the same distance to the sensor. The vertical front wall and the surface area in front of the building compose a corner reflector resulting in the bright double-bounce effect b. The scattering area that is only characterized by scattering from the roof is denoted by d. The elevated building occludes parts of the surface behind the building from the radar beam, resulting in the shadow area e. This backscattering profile is flexible with respect to a number of parameters. For instance, for very high buildings, there is typically no area d as the part of the roof is entirely included in the layover area. In fact, both the layover and the shadow areas of the footprint are partially masked by the trees that surround the building. For gable-roof buildings, the theoretic scattering signature is slightly different. The signature has a second bright scattering feature acd at the sensor close side resulting from direct backscattering from the roof. The extent and the strength of this feature depend on the relationship between θ and the roof inclination angle α. For α = θ, the strength of this feature is maximum, whereas its extent is minimum. Moreover, we found that in actual 1-m-resolution TerraSAR-X and Cosmo-SkyMed data, this second bright scattering area is also detectable for buildings with a high aspect angle. Where we show actual scattering signatures from gable-roof buildings with small and large aspect angles, respectively.
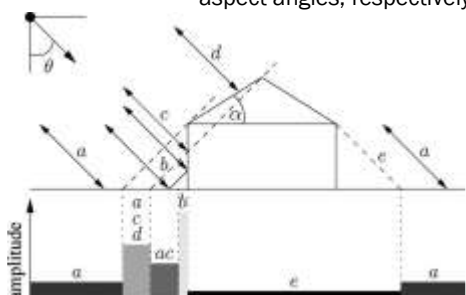


**Fig. 2:** Scattering model for a gable-roof building with viewing direction from left.

………………………………………………………………………………………

The double-bounce feature is very pronounced. A detailed analysis of the characteristics of the double bounce of buildings with actual TerraSAR-X data and theoretic electromagnetic scattering models presented in showed that this feature has a significant dependency on the building aspect angle. The double bounce has a strong signature for buildings with low aspect angles. Then, it decays significantly in a narrow range of aspect angles, while it drops moderately for larger aspect angles. The method presented in this work will take into account this nonlinear relationship between the strength of the double bounce and the aspect angle shown in [Fig. 2].

## RESULTS AND DISCUSSION

### Preprocessing and feature extraction

In the preprocessing, the input image is first radiometrically calibrated. Although this step is not strictly necessary, it permits to define the algorithm parameters to be used with SAR images of different data sets and data products acquired by either the same or different sensors. Afterwards, the image is filtered with a Gamma MAP filter in order to reduce the signal variability due to speckle. Both the unfiltered and filtered images are used by the algorithm. The basic features composing building radar footprints in VHR SAR images are extracted from the calibrated image. According to the aforementioned assumptions on building shapes, these are bright linear features with different thicknesses, and dark areas. The former

113

are usually related to double-bounce scattering or, as the line thickness increases, to layover areas, where the roof or the facade scattering may be dominant depending on the building characteristics. The latter are due to building shadows and low-return areas. These features are sufficient to describe the main parts of a building radar footprint in meter-resolution images shown in [Fig. 3].
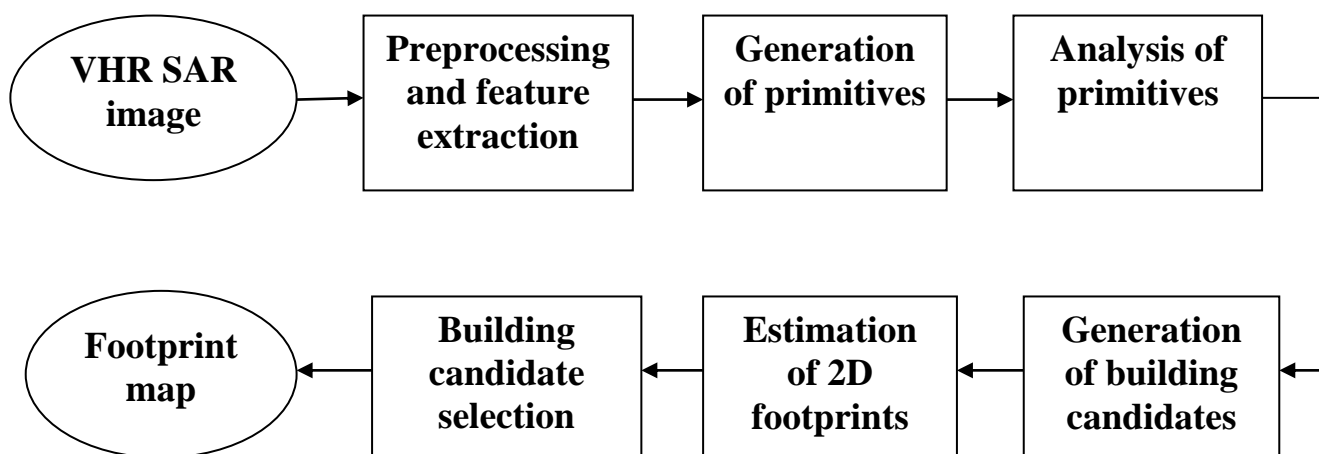
**Fig. 3:** Block scheme of the processing chain of the reconstruction of building radar footprints in single VHR SAR images.
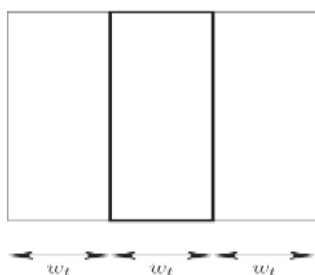
...................................................................................................................

**Fig. 4:** Definition of the window used by line detector.

...................................................................................................................

## Extraction of bright linear features

The extraction of bright linear features is performed on the unfiltered image by means of the line detector. This detector is based on a three-region sliding-window approach and is a well-known algorithm specifically developed for SAR images. In this project, we use as reference for the window size the dimension of the central region, and assume that the lateral regions have the same width and length. The length has been set to ten times the resolution of the image, and 16 directions have been considered for the window. As we are interested in both thin and thick linear features, the detector is applied T times with different increasing window sizes shown in [Fig. 4].

$$W_t \ (t = 1, \ldots, T) \qquad [1]$$

Each filtering is performed independently. The result of each filtering is a detection map, which is then threshold, obtaining binary linear regions which thickness is related to wt. Such regions are vectorized using a rectangular approximation. This is performed by approximating the region skeletons with lines and using such lines as the axis of rectangles of width wt. An example of the detection on a meter-resolution SAR image of an urban area using wt = 5 m. The intermediate results are also shown. For each rectangle r, the local contrast Value Cr is calculated on the filtered image as shown in [Fig. 5].
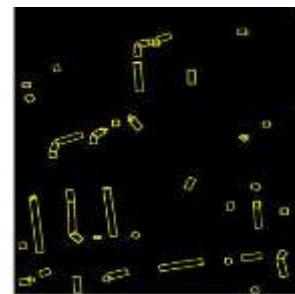
**Fig. 5:** Meter-resolution TerraSAR-X image of an urban area. **Fig. 6:** Result of the line detection using wt = 5 m.

......................................................................................................

As a result of the T filtering, we obtain T vector maps containing rectangles corresponding to bright linear features with different thicknesses. These maps are thus merged in one map. It is possible that the same real bright objects are detected independently for different wt, resulting in overlapping rectangles in the merged map shown in [Fig. 6]. In order to reduce the number of rectangles, a down selection step is performed by means of a production net shown in [Fig. 7, 8]. For each combination of two rectangles (i, j), the net tests the following conditions:

    1) The width of the two rectangles is similar, and

    2) The two rectangles overlap.

Condition 1) is met when

$$|wi - wj| < \delta wmax \quad [2]$$

where wi and wj are the widths of the rectangles, and δwmax is a user-defined threshold.

Condition 2) is fulfilled when

$$A\cap > Ai \cdot At \wedge A\cap > Aj \cdot At$$

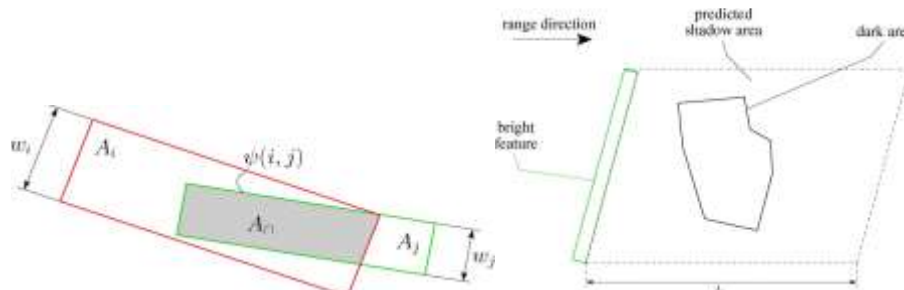where Ai and Aj are the areas of the rectangles, A∩ = Ai ∩ Aj.



**Fig. 7:** Measures involved in the rectangle down selection **Fig. 8:** Predicted shadow area and selected dark area

......................................................................................................

### Extraction of dark areas

Dark areas are extracted from the unfiltered image by means of mean shift clustering followed by a threshold operation. This operation selects only the clusters with amplitude values lower than a user-defined threshold. The extracted clusters are then vector zed, and a simplification procedure is applied in order to reduce the number of vertexes describing their shape. Such simplification is not strictly necessary, but it allows the algorithm to work with simpler objects reducing the needed amount of memory. In order to select only the dark regions which are likely to be related to building shadows, the algorithm removes the regions which are not located in the sensor-far side of any bright linear feature. This is done by keeping only the dark areas which overlap with the predicted shadow area of the bright features. The predicted shadow area is determined by taking into account the viewing configuration of the SAR. The maximum range size ls of the expected shadow area is set by the user. The parameters of the mean shift clustering and the value of xs have to be selected by analyzing the amplitude of sample pixels belonging to shadow regions in the SAR image.

## Generation of primitives

The goal of this step is to generate the primitives that will be used in the following steps as basis for the composition of building radar footprint hypotheses. Starting from the set of simple extracted bright linear features and dark areas, the algorithm merges adjacent features in order to compose bigger objects. This is done by a production system applied to the vector domain, after a conversion from slant range to ground range, and is aimed at compensating for errors in the feature extraction step shown in [Fig. 9]. The conversion from slant to ground range allows us to define the parameters of the method in the ground domain, which is independent on the incidence angle and thus simpler to handle for an end-user. After their generation, composed objects are given as input to the production system. Therefore, multiple compositions with other simple or composed objects are possible. The set of objects and productions involved in the generation of primitives. The composition of dark areas is described by the production rules P1 and P2. Such rules merge two dark areas when these are adjacent. In this project, the merging is carried out by calculating the convex hull including the two original features.
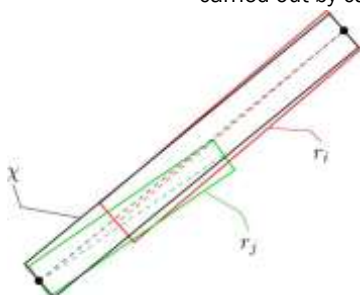
**Fig. 9:** The merging of two rectangles.

...................................................................................................

For the case of bright linear features, merged features are generated as new rectangles that have as principal axis the conjunction of the two extremes of the principal axes of the original features which have the largest relative distance.

The algorithm merges two bright features when the following conditions are fulfilled:
1) The features have similar widths,
2) Their orientation is approximately the same,
3) The composed object has an orientation that is approximately the same of the original features.

Condition 1) is equivalent to (2). Condition 2) is fulfilled when

where $\psi(i, j)$ is the angle between the two linear bright features represented by the rectangles $i$ and $j$ and $\delta\psi max$ is user-defined and indicates the maximum angle allowed between two features for which they are considered parallel. The value of $\delta\psi max$ should be on the order of $20\circ$.

Condition 3) is satisfied when

where $\chi$ is the rectangle corresponding to the composed bright linear feature. It is probable that in this step, many bright primitives are generated. In order to reduce their number, a selection procedure as the one described in the previous subsection for bright linear features can be applied. At the end of this step, for the whole set of simple and composed objects, the algorithm stores a set of attributes regarding their size and position, and the amplitude features of the composing pixels.

## Analysis of primitives

This step aims at evaluating the semantic meaning of the primitives. Here, we use the term semantic meaning to describe the membership grade of a certain primitive to belong to a predefined scattering class. Different scattering classes are related to different parts of building radar footprints. The choice of the set of semantic classes is related to the types of features extracted from the image and, thus, to the image resolution. For bright primitives, we define four semantic classes: general line, double bounce, roof, and facade. For dark primitives, only the class shadow has been defined. The membership grade of each primitive to belong to a certain semantic class is calculated on the filtered image according to membership functions (MFs) derived empirically for each semantic class.
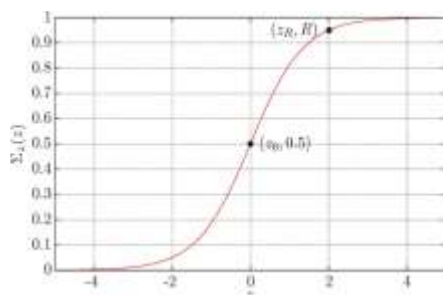
**Fig. 10:** Sigmoid function Σz(z) defined

.......................................................................................................

The MFs are defined as a product of sigmoid functions. Each sigmoid factor depends on a specific attribute of the primitives. The function Σz(z) gives values in the range (0, 1). For each sigmoid function, two parameters need to be specified: the value of z for which the sigmoid returns a high likelihood $R(z_R)$, and the value corresponding to the center of the sigmoid ($z_0$), implicitly setting the slope of the function. The MFs, which relate bright primitives to the relative semantic classes, are defined according to the tree. The number of sigmoid functions composing the MF for a semantic class is smaller or equal to the number of branches that connect the root to the final leaf. In the following, we describe in detail the MFs of each semantic class for both bright and dark primitives, by also suggesting the range of parameters that is most suited for the related scattering class. Unless otherwise stated, such values have been estimated by analyzing the scattering properties of a set of samples of the considered scattering classes manually selected on the meter resolution TerraSAR-X input images used in this paper shown in [Fig. 10]. As the images are calibrated, the suggested values related to pixel amplitude can be considered generally valid. In the case of images acquired at different resolution and or with a sensor with different characteristics, some of the values should be estimated again.

## Bright primitives
### General line

The membership grade of a primitive to the class general line depends only on its width. It gives a measure of the membership of the primitive to the high-level class thin line, which depends on the primitive width w.

### Double bounce

The double-bounce effect appears in VHR SAR images as relatively thin bright lines. It is more evident when the building wall is parallel to the azimuth direction, i.e., its aspect angle is close to zero. In such a case, the MFs of the classes general line and double bounce give very similar values. Such values have been chosen according to our previous studies about the double bounce effect in VHR SAR images.

### Roof

The class roof is the most specific, as it appears as leaf for every branch combination. This is due to the intrinsic uncertainty given by the fact that we are using only one VHR SAR image and that we are considering meter-resolution images. Indeed, the signature of a building roof could be either a thin line or a homogeneous rectangular area, or a non-homogeneous rectangular area. Therefore, for the class roof, the final membership grade is calculated as the maximum of the membership grades given by the three MFs corresponding to the three occurrences of the class in the tree. These refer to the homogeneity of the pixels contained in the primitive. The homogeneity is measured using as parameter the coefficient of variation σ of the pixels.

### Facade

As reported in the tree, the semantic class facade includes primitives with a relevant width and which pixels have non-homogeneous values.This is the general scattering behavior of building facades, where returns coming from structures like windows or balconies give a strong textured signature in the radar footprint. As a further constraint, the aspect angle of the building should not be too high. Indeed, the facade scattering area in the radar footprint becomes smaller with increasing aspect angles shown in [Fig. 11].
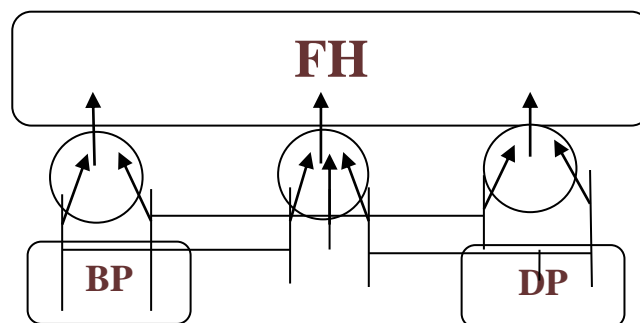
**Fig.11:** Production net for the generation of building radar footprint hypotheses

······································································································

### Dark primitives

For dark primitives, only the semantic class shadow has been defined. The MF of this class takes into account the mean and the coefficient of variation of the pixels contained in the primitive. The MF is tuned in order to penalize dark primitives with high mean value and high coefficient of variation.

### Two-dimensional reconstruction

The 2-D radar footprint reconstruction aims at refining the detection of both, the bright part and the dark part (if present) of the footprint hypotheses selected in the previous step. This is performed in order to reduce the effect of imprecision coming from the feature extraction and primitive generation steps, and to provide reliable outputs which can be used as a starting point to estimate parameters of the buildings, such as their length, width, and height (with the limitations imposed by the fact that only a single image is available). The result of this procedure is thus the final map of the building radar footprints detected and reconstructed from the input VHR SAR image. As a first step, the algorithm generates for each footprint hypothesis a best-fit rectangle which includes its bright primitives. If only one bright primitive is present, the best-fit rectangle and the bright primitive match. Then, the rectangle is translated, rotated, expanded, and shrunk with the goal to maximize Cr. The maximization is carried out using a particle swarm optimization approach, which is a well-known iterative method suited for the optimization of problems without a priori assumptions. A similar approach was applied in for binary images and using a different optimization strategy. The rectangles which become smaller than the minimum sizes set in the previous steps of the algorithm are deleted. Moreover, it is possible that some rectangles move and overlap. Therefore, the algorithm deletes overlapping rectangles, and thus the corresponding footprint hypotheses, keeping only the rectangles associated to the hypotheses with the highest scores Sh. A refinement procedure is carried out also for the dark part of the footprint hypothesis, when it is present. In fact, a good knowledge of the size of the shadow area of a building can be exploited for the retrieval of the building height. The refinement aims at expanding the dark primitive on pixels with amplitude values similar to those of shadows in the sensor far side area of the reconstructed bright primitives. To this end, the center of the dark primitive is used as seed for a region growing algorithm which, starting from an initial circular contour, stretches its border to fit the dark area around the seed. The chosen implementation is a level-set algorithm which moves the contour by including the pixels which have amplitude values in the range [0, mSR]. The resulting regions are cut in the azimuth direction in order to match the extension of the reconstructed bright part of the footprint hypothesis. Indeed, the reconstructed regions are associated to building shadow areas, which cannot be larger than the corresponding buildings in the azimuth direction. The size of the reconstructed dark areas in the range direction depends only on the radiometric measurements in the image. As the proposed technique uses as input only one VHR SAR image and no a priori information is available, it is not possible to detect the end of the shadow region by other means. This may lead to shadow areas which are longer than real shadows because of low scattering areas behind the buildings (e.g., roads, parking lots). This problem can be partially mitigated by imposing a maximum shadow range size IS set by the user. Shadows longer than IS are cut to IS, and a flag is set to notice the user about the lower reliability of the reconstructed shadow.

### EXPERIMENTAL RESULTS

In this section, we show the results obtained by applying the proposed methodology to a real meter-resolution large SAR image. After a brief description of the used data set, we show and analyze qualitatively the results obtained on the whole image following the grid-computing approach described. Then, we focus on two subsets of the image in order to assess quantitatively the accuracy of the method.

## Data set description

The effectiveness of the proposed method has been tested on a TerraSAR-X image of the city of Dorsten, Germany. The image has been acquired in HH polarization in spotlight mode, resulting in a geometrical resolution of approximately 1.1 m × 1.2 m (azimuth × slant range). The incidence angle varies between $50.3°$ and $51.0°$. The original scene has been cut to a subset of 2800 × 3712 pixels, covering an area of approximately 10 km2. The cut includes both urban and rural areas. Urban areas are characterized by both flat- and gable-roof buildings at various settings. The SAR test image and an optical image corresponding to the same area taken from Google Maps.

## RESULTS ON SUBSET 1

The values of such parameters have been chosen according to the guidelines in table 1. The results obtained are shown in Fig. 12. The method shows in overall a high detection rate. False alarms are mostly related to the scattering from objects different from buildings (e.g., trees, garages) that show radar footprints similar to those of buildings.

**Table 1:** Parameters used in the feature extraction and primitive generation steps in the experiments carried out with the proposed

| Parameter | Value |
|---|---|
| T | 7 |
| $w_1, \ldots, w_7$ | 3,5,….,15 |
| Wmax | 3 |
| At | 0.5 |
| Xs | -12.2db |
| Ls | 30m |
| Ψmax | 20° |

A particular case is represented by bridges, which have been also detected. Such structures can be easily masked, either using a priori information about the presence of rivers, or by extracting the rivers directly from the SAR. The radar footprints of complex buildings which do not correspond to the rectangular model used in this project are mostly detected with some reconstruction errors. In general, the proposed method detected and reconstructed quite precisely the radar footprints of medium- and big-size buildings that fulfill the rectangular model. Radar footprints of small adjacent buildings aligned in regular patterns are also detected, but in some cases are considered as belonging to a single building. Small buildings which do not show clear features are not detected by the method. However, considering the use of a single SAR image, the results can be considered qualitatively very satisfactory. Moreover, it is worth noting that if the proposed method is applied in order to derive indexes of the presence of buildings, reconstruction errors do not represent a critical issue shown in [Fig. 13].



**Fig. 12:** Original TerraSAR-X image of the considered area, viewing direction from left

**Fig. 13:** Reconstructed building radar footprints on the SAR image

**Table2.** Algorithm Performance for subset 1, subset 2

| | Building size | Number of buildings | Detected | False alarms | Split | Merged |
|---|---|---|---|---|---|---|
| **Subset 1** | Large | 21 | 19 | 0 | 2 | 1 |
| | Medium | 26 | 22 | 2 | 4 | 3 |
| | Small | 66 | 35 | 9 | 1 | 9 |
| **Subset 2** | Large | 12 | 12 | 0 | 4 | 0 |
| | Medium | 27 | 23 | 2 | 4 | 3 |
| | Small | 53 | 34 | 9 | 1 | 8 |
| **Subset 1+2** | Large | 33 | 31 | 0 | 6 | 1 |
| | Medium | 53 | 45 | 4 | 8 | 6 |
| | Small | 119 | 69 | 18 | 2 | 17 |

## RESULTS ON SUBSET 2

This area is characterized by a large number of trees locate dalong the streets. Such trees often mask the radar returns also from medium-sized buildings. Moreover, small buildings are usually quite irregular and show many structures on their walls. This subset is thus a challenging benchmark for the proposed technique. Table reports the results obtained for the subset 2, shows the correct and missed detections on theoptical image. As for the subset 1, the detection rate for the classes large and medium is very good. For the class small, performances are less satisfactory. The number of split buildingsis 1 for the class small, 4 for the class medium, and 4 for the class large; while the number of merged buildings is 8 for the class small, 3 for the class medium, and 0 for the class large. The total number of false alarms is 11. As for subset 1, the most of them are related to small false building radar foot prints. In overall, considering the issues mentioned at the beginning of this paragraph and the limited amount of information used by the proposed technique. The results can be considered very good. In order to provide a more general view of the results obtained by the proposed method, Table II also reports the overall results computed by summing the results of the subsets 1and 2. The total statistic confirms the trend highlighted for the single subsets, i.e., the algorithm has a high detection rate for medium and large buildings, with a limited amount of false alarms, whereas its performance decreases in the case of small buildings, which are associated to most of the total number of false alarms. It is worth noting that it is possible to mitigate this problem by imposing a rule for discarding the footprints smaller than a user-defined minimum footprint size. As a consequence, the number of false alarms would be considerably reduced and the detection of radar footprints of small buildings would not bea target of the method anymore. This is a reasonable strategy to adopt for tuning the proposed technique only on the detection of medium and large buildings.

### Selection of algorithm parameters

The tuning of the parameters has been performed according to the scene investigated. However, some parameters are not strictly related to the image analyzed and can be set a priori following general rules. Moreover, many of the considered parameters have a clear physical meaning that helps the user to include its prior knowledge on the scene in the detection algorithm. In addition to the guidelines already provided, in this section, we analyze more in detail the role of the parameters of the proposed method.

### Feature extraction and primitive generation

In these steps, the main parameters of the proposed technique are related to the detection and generation of bright rectangles, and to the extraction of the shadows. The possible range of values for the window of the line detector $wt$ should be set between the expected thickness of thin linear features and the maximum size of the buildings which has to be extracted. The sampling of the range of $wt$, given by the number of filtering T, should assure that most of the linear features can be effectively modeled with the considered values of $wt$. The minimum value for $\delta wmax$ has to be greater than the width sampling resulting from the definition of the values of $wt$. On the one hand, a value smaller than this quantity would not allow the algorithm to down select effectively the rectangles produced in the feature extraction step. Moreover, the procedure for the generation of primitives would combine only rectangles with approximately the same width. On the other hand, a value much greater than the width sampling would make the algorithm to down select too many rectangles, and combine features with much different widths. According to our tests, a good choice for the value of $\delta wmax$ is 1.5 times the width sampling used in the line detection. Regarding the parameters At and $\delta \psi max$, high values for At and low angles for $\delta \psi max$ make conditions (3) and (4) too stringent, respectively.

### Analysis of primitives

In this step, the main parameters to be set are those related to the MFs defined for the different scattering classes. The choice of the value of R is not critical, and R = 0.999 can be considered as a fixed

value. The parameters wthin R = wthick R , wthin 0 , and wthick 0 used in this project can also be considered general. Indeed, they are given in meters, so that they do not depend on the resolution of the system. According to our tests, setting wthin R = wthick R to a value 2–3 m greater than the expected thickness of the linear signatures due to the double-bounce effect gives the best results, as the procedure which creates rectangles from the output of the line detector may overestimate their actual thickness.

### Selection of hypotheses and 2-D radar footprint reconstruction

The parameter Nh is related to the reliability assigned by the user to the footprint hypotheses composed by only two primitives. In our tests, by setting this parameter to higher values resulted in detection maps with less hypotheses composed by three primitives, as expected. Indeed, increasing the value of Nh makes three-primitive hypotheses to have higher probability to score lower than those composed by two primitives. Therefore, three primitive hypotheses have higher probability to be discarded when they overlap with others made up of two primitives. This does not affect significantly the detection rate of the proposed method, but it increases the probability that the extracted footprints are not well-reconstructed (e.g., shadows are missing even though they were detected). On the contrary, by setting Nh to low values would increase the number of missed detections.Therefore, the choice of Nh should be done by the user as atradeoff between reliability of the reconstruction and detectionperformance.The pair of parameters (δdR, δd0) and (δψR, δψ0) are relatedto the vicinity and relative orientation of the primitives, respectively.The values proposed in this project can be considered general for the defined scattering classes. Note that, using these values, the sigmoid functions present are quite smooth, thus mitigating the effect of possible errors in feature extraction. The last parameter to be discussed is Sh, min. This parameter gives the tradeoff between false and missed detections. According to our tests, the use of high Sh, min results in a greater number of missed detections, as expected. However, the number of false alarms is not reduced significantly. Indeed, these are usually related to footprints of other man-made structures, or trees, which actually appear as related to buildings. For this reason, values in the order of 0.6–0.7 are suggested.

### Computational load

The test image described in Section V-A has been processed using a cluster composed by 16 AMD Opteron 6172 CPUs, for a total of 192 cores, with 4 GB of RAM per core. The image has been split on tiles of 300 × 300 pixels with an overlapping offset of 30 pixels with the neighbors. The total number of tiles was thus 154, and each tile was processed by one core. The total processing time was about 45 min. With the same infrastructure, it is thus possible to process a whole spotlight image of about 6000 × 10.000 pixels in less than 3 h. We also tested the proposed technique using a smaller cluster composed by eight commercial workstations equipped with Intel Core i7-870 quad-core processors and 8 GB of RAM. The total processing time for the test image on this smaller architecture was about 1 h and 30 min, which is a good performance in terms of operational application of the algorithm.

### Input Image

We present a novel method for automatic building detection, which also reconstructs the 2D radar footprint of the detected buildings. The method is based on the extraction of a set of low-level features from the images and on their combination in more structured primitives. In order to process large VHR SAR images, the method has been implemented on a computer cluster. We demonstrate the effectiveness of the method using a large Terra SAR-X spotlight scene. In order to exploit this information in different application scenarios, robust building detection and reconstruction methods are essential. Different techniques for building detection and reconstruction from VHR SAR. They mainly rely on the availability of multi-modal data that require multiple acquisitions with different viewing configurations shown in [Fig. 14].



**Fig. 14:** Selecting input image.

....................................................................................................

121

In the preprocessing, the input image is first radio metrically calibrated. Although this step is not strictly necessary, it permits to define the algorithm parameters to be used with SAR images of different data sets and data products acquired by either the same or different sensors. Afterwards, the image is filtered with a Gamma MAP filter in order to reduce the signal variability due to speckle. Both the unfiltered and filtered images are used by the algorithm. The basic features composing building radar footprints in VHR SAR images are extracted from the calibrated image. According to the aforementioned assumptions on building shapes, these are bright linear features with different thicknesses, and dark areas shown in [Fig. 15].



**Fig. 15:** Preprocessed output image.
..................................................................................................

This step aims at evaluating the semantic meaning of the primitives. Here, we use the term semantic meaning to describe the membership grade of a certain primitive to belong to a predefined scattering class. Different scattering classes are related to different parts of building radar footprints. The choice of the set of semantic classes is related to the types of features extracted from the image and, thus, to the image resolution. For bright primitives, we define four semantic classes: general line, double bounce, roof, and facade. For dark primitives, only the class shadow has been defined. For dark primitives, only the semantic class shadow has been defined. The MF of this class takes into account the mean and the coefficient of variation of the pixels contained in the primitive. The order in which the bright primitives are aggregated is also taken into account, at least two hypotheses will be generated for each pair of bright primitives shown in [Fig. 16].



**Fig. 16:** Primitive detection process.
..................................................................................................

The 2-D radar footprint reconstruction aims at refining the detection of both, the bright part and the dark part (if present) of the footprint hypotheses selected in the previous step. This is performed in order to reduce the effect of imprecision coming from the feature extraction and primitive generation steps, and to provide reliable outputs which can be used as a starting point to estimate parameters of the buildings, such as their length, width, and height. The result of this procedure is thus the final map of the building radar footprints detected and reconstructed from the input VHR SAR image. The size of the reconstructed dark areas in the range direction depends only on the radiometric measurements in the image. As the proposed technique uses as input only one VHR SAR image and no a priori information is available, it is not possible to detect the end of the shadow region by other means. This may lead to shadow areas which are longer than real shadows because of low scattering areas behind the buildings shown in [Fig. 17].
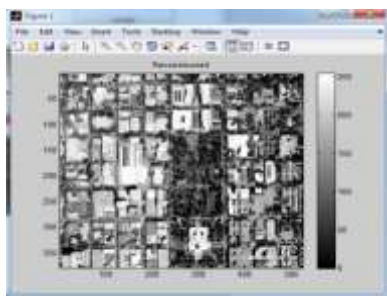
**Fig. 17:** Reconstructed image.

.........................................................................................................

# CONCLUSION

In this paper, the problem of the detection and reconstruction of building radar footprints in VHR SAR images has been addressed. It extends state-of-the-art feature extraction and composition steps to more structured primitives using a production system and by introducing the concept of semantic meaning. This has been done in order to compensate for the lack of information due to the fact that only one VHR SAR image is used as input. It allows the technique to select the most reliable primitives and footprint hypotheses during its processing steps. As a further refinement; the proposed technique also reconstructs the detected radar footprints. The goal of this step is to provide as output a map which can be used as a starting point for further calculations. Moreover, by exploiting the reconstruction of the shadow areas, height retrieval techniques can be also applied to estimate building heights. To make it possible to use the proposed technique on large VHR SAR images in near real time, we also proposed and implemented an infrastructure based on a computer cluster for the processing of large VHR SAR scenes. The system can be programmed in integrated chip and can be inhibited into the camera itself, so that real time detection can be achieved. The threshold value which has been calculated manually in the process based on the approximate median of the object intensity can be automated in future for higher efficiency. More effective threshold techniques can be implemented for low quality videos which would help satellite surveillance applications.

# CONFLICT OF INTEREST
There is no conflict of interest.

# ACKNOWLEDGEMENTS
None

# FINANCIAL DISCLOSURE
None

# REFERENCES

[1] AUTOMATIC DETECTION AND RECONSTRUCTION OF BUILDING RADAR FOOT PRINTS FROM SINGLE VHR SAR IMAGES " Adamo Ferro, Dominik Brunner, and Lorenzo Bruzzone, IEEE Transactions on geosciences and remote sensing, 61(2), February 2013.

[2] BUILDING RECONSTRUCTION FROM SAR IMAGES AND INTERFEROMETRY" Franz W. Leberl, Regine Bolter, IEEE Transactions on geosciences and remote sensing, May 2012.

[3] RECONSTRUCTION OF BUILDING FROM VHR SAR AND OPTICAL DATA BY USING OBJECT ORIENTED IMAGE ANALYSIS" Namhyum Kim , February 2011.

[4] BUILDING DETECTION AND RADAR FOOTPRINTS RECONSTRUCTION FROM SINGLE VHR SAR IMAGES" Adamo Ferro, Dominik Brunner, and Lorenzo Bruzzone, March 2011.

[5] AntoBennet M, JacobRaglend. [2012] Performance Analysis Of Filtering Schedule Using Deblocking Filter For The Reduction Of Block Artifacts From MPEQ Compressed Document Images, Journal of Computer Science, 8( 9):1447-1454,

[6] AntoBennet M, JacobRaglend. [2011]Performance Analysis of Block Artifact Reduction Scheme Using Pseudo Random Noise Mask Filtering", European Journal of Scientific Research, 66 (1):120-129

[7] AntoBennet M , Resmi R. Nair, Mahalakshmi V, Janakiraman G. [2016] Performance and Analysis of Ground-Glass Pattern Detection in Lung Disease based on High-Resolution Computed Tomography, Indian Journal of Science and Technology, 9(2):1-7

[8] AntoBennet M, JacobRaglend. [2012] 'A Novel Method Of Reduction Of Blocking Artifact Using Machine Learning Metric approach', Journal of Applied Sciences Research, 8(5):2429-2438.

Editor: Dr. K. Sakthisudhan

THE IIOAB JOURNAL